Journal of Hazardous Materials, 14 (1987) 213—232
Elsevier Science Publishers B.V., Amsterdam — Printed in The Netherlands

EXPANSION AND EVOLUTION OF HEAVY GAS AND PARTICULATE CLOUDS

R.J. BETTIS, G.M. MAKHVILADZE* and P.F. NOLAN

Department of Chemical Engineering, South Bank Polytechnic, London SE1 0AA (Great Britain)

(Received April 23, 1985; accepted in revised form April 28, 1986)

Summary

Physical and mathematical models have been applied to stages of two phase releases following the failure of pressurised vessels. The initial expansion stage has been modelled using an experimental apparatus involving the measurement of pressure versus time and of Freon-11 aerosol particle sizes and velocities. An analysis of the experimental data combined with an appreciation of the thermodynamics has allowed estimations of the time dependent processes. The analytical description of the critical pressure decrease on the opening of the vessel is given.

The later evolution stage has been mathematically modelled by assuming that the two phases have separate velocities. The cloud motion characteristics have been shown to depend upon the degree of hydrodynamic interaction between the particles via the gaseous phase. For small particle fractional volumes, this interaction is small and each particle behaves as a single particle corresponding to a "filtration" regime. However, for larger concentrations the air between the particles becomes entrained due to the particle motion and the cloud velocity exceeds that of the single particle. In this "entrainment" regime large scale vortex motion occurs. The cloud is transformed either into two cylindrical vortices for planar symmetry or into a toroidal vortex for axial symmetry. The regime of the cloud motion defines the sedimentation characteristics of the particles.

Introduction

Despite continuous efforts by scientists and engineers [1—9] problems still remain with regard to the prevention of explosions following the failure of pressurised storage vessels. Emphasis has been placed on the storage and transportation of liquid petroleum gas (e.g. propane, butane). Such substances require the maintenance of an increased pressure in the vessel simply because their boiling points at normal pressure are lower than ambient temperatures (e.g. the boiling point for propane is −45°C (228 K) at 1 bar). In order to store propane as a liquid at, say 20°C (293 K) a pressure

*Present address: Institute for Problems in Mechanics, USSR Academy of Sciences, Prosp. Vernadskogo 101, Moscow 117256, U.S.S.R.

of 10 bar must be applied. Such storage under pressure increases the risk of explosion due to vessel failure [1, 2, 5, 7].

The failure of a vessel, is accompanied by an abrupt reduction in pressure, the liquid becomes superheated, rapidly vaporises, and a mixture of vapour and liquid is released from the vessel. The cloud formed as this release mixes with the surrounding air is highly dangerous, both from the potential environment effects of the spreading of these materials and also from the possibility of a flammable mixture being ignited. If ignition of the release takes place, either at the vessel or in the spreading cloud, a major explosion can occur, causing the destruction of surrounding building and plant as well as possible loss of life.

Similar examples can follow damage to pressurised chemical reactors. The failure of reactors may not only allow the discharge of gases and liquids but, additionally, solid particles.

Previous work on catastrophic vessel failure [1, 3, 4] has assumed that the expansion is independent of the vessel, i.e. the assumption has been that the vessel has been completely and instantaneously removed leaving a body of superheated liquid. In incidents, this is not the case and this work assumes that some interaction with the vessel fragments occur.

Effective methods for the prevention of such incidents can only be developed as a result of detailed analysis of the physical phenomena accompanying such releases. Both gas dynamics and hydrodynamics are involved in a liquid petroleum gas (LPG) release. These cover the formation of pressure waves, multicomponent flow, i.e. vapour, liquid droplets and entrained air, both inside the vessel and after its escape, the subsequent evolution of the cloud above the vessel including increase in size, the air entrainment, the drifting of the cloud due to bulk air motion (wind) and the "rain out" of droplets under gravity. Similar processes would occur following the failure of a pressurised chemical reactor.

It is desirable to have an understanding of the processes to provide some simple, reliable relationships, either empirical or theoretical, to permit the estimation of the parameters of the cloud from a possible release. The present study incorporates both experimental and theoretical investigations.

The experimental work has provided pressure histories of the vessel following failure, average droplet sizes, overall cloud expansion rates and cloud profiles for different cases of initial pressure and initial mass of liquid. The theoretical work has concerned the cloud evolution under gravity.

Experimental work — The initial expansion

The aim of the experimental work was to simulate the first phase of a pressurised liquid release, during which the pressure falls to that of the surroundings. The model material was Freon-11, which has a normal atmospheric boiling point of c. 22°C (295 K) and was chosen for its relatively inert nature and ease of handling. These experiments have a direct

significance for releases involving liquids whose normal boiling point is above the ambient temperature, but which are being processed under pressure at temperatures in excess of their normal boiling points. The experiments also provide a foundation for the study of liquids held under pressure at ambient temperatures in excess of normal boiling points.

The release was produced by "failing" a fully instrumented vessel consisting of two hemi-spheres held together pneumatically and containing the model material maintained at measured internal pressure, temperature and fill-level. The assembled vessel is 114 mm in diameter, and has a maximum fill of 1.1 kg of Freon-11. A heater in the vessel allows energy to be put into the closed system, increasing the temperature and pressure of the Freon-11. When the appropriate release conditions had been established (the attainment of an equilibrium state at a chosen internal pressure), the pressure on the pneumatic system holding the vessel together was reversed, and the two halves pulled apart.

The resulting release consisted of three parts:

(i) Vapour; produced during the rapid boiling as the pressure was reduced.

(ii) Aerosol; the liquid broken up during boiling and entrained into the expanding vapour, which carried it away from the release point. The size of the droplets which form the release was measured using a laser diffraction system, and also by flash photography. The profile of the spray, and its overall velocity was examined using video and high speed cine photography.

(iii) Bulk liquid; any liquid which remained in the immediate vicinity of the release point. This was collected on a tray below the vessel. The tray was mounted on a balanced load cell system, allowing measurement of the weight of liquid.

Preliminary results are presented in Table 1. They are average values from several experiments.

The droplet sizes (the mean sizes of the best log—normal distribution) were measured at a point level with the centre-line of the vessel, at a distance of 0.5 m from the centre. The velocity estimates were average values over the first two metres of travel away from the vessel. The time given as release time was the time for equalisation of vessel internal pressure with the atmosphere. This was measured using a pressure transducer system in conjuction with a transient recorder to capture this rapid event for later analysis.

The time required for pressure equalisation (100 ms) is greater than the theoretical time (0.1 ms) based on the sonic velocity in the liquid. This greater time is due to the confinement by the walls of the vessel.

The theoretical flash fraction can be obtained and the amount of residual liquid measured. This allows the amount of aerosol to be found by difference from the original fill-level.

For simplicity, in calculations for the later stage of evolution the mean

TABLE 1

Results from experimental work

Pressure (kPa)	Fill-level W (g)	Release time t_e (ms)	Droplets		Residual liquid (g)
			size (μm)	velocity (m s^{-1})	
310.3	1000	225	80		289
310.3	750	222	82		246
310.3	500		85	6.7	
310.3	300	97	90		178
413.7	500				70
413.7	300				45
482.7	500			12.8	
517.2	1000				103
206.9	500			4.5	

droplet size was taken as 100 μm. The characteristic velocity of the spray was 10 m s^{-1}. The subsequent stage of cloud evolution was not studied experimentally, due to space restrictions.

Thermodynamic analysis — Initial expansion

In order to complete the study of the initial expansion, it is necessary to carry out an analysis based on thermodynamics. Hardee and Lee [1] suggested such an approach in their study of LPG storage. A three stage model was proposed.

During the first stage, the pressure in the vessel decreases until it is equal to that of the surrounding atmosphere. An isentropic expansion was assumed and the system parameters determined as functions of the actual pressure. The functions correlated well with presented experimental results. Hardee and Lee [1] also produced a theoretical time dependence for the pressure, although the basis of these calculations is not described. A number of additional assumptions would be required to be made for such calculations.

The second stage comprises the complete emptying of the vessel and the assumption of constant total momentum can be questioned.

The third stage described the radial evolution of the cloud in a horizontal plane, while assuming no motion in the vertical plane. Assuming constant total momentum the cloud radius is time dependent. However, such a dependence may be questioned because of the use of simplistic models to describe the complex physical situation.

Following the pressure drop caused by vessel failure, the thermodynamic equilibrium is regained by flash boiling. The standard approach to this is to assume an isentropic phase change. Since all the energy required is present in the superheated liquid, the process is also adiabatic, until vapour expansion causes work to be done on the surroundings.

Following the example set by Hardee and Lee [1], the initial expansion is considered isentropic, thus

$$S_t = X_t S_{1t} + (1 - X_t)\, S_{2t} = \text{a constant} \tag{1}$$

hence

$$S_i = X_i S_{1i} + (1 - X_i)\, S_{2i}$$
$$= X_t S_{1t} + (1 - X_t)\, S_{2t} \tag{2}$$

i.e.

$$X_t = \frac{(S_{2i} - S_{2t}) + X_i\,(S_{1i} - S_{2i})}{(S_{1t} - S_{2t})} \tag{3}$$

On the assumptions that the vapour behaves as an ideal gas

$$\rho_{1t} = \frac{P_t m}{R T_{1t}} \tag{4}$$

and that the vapour temperature is a constant and equal to the room temperature, the vapour volume is given by

$$V_{1t} = \frac{X_{1t} W}{\rho_{1t}} \tag{5}$$

Thus, if the relationships between entropy and pressure are known, then the pressure dependencies of quality, vapour density and vapour volume can be calculated. Pressure—entropy relationships were taken from curves fitted to data from standard tables [10]. The accuracy of the fitted curves, over the range considered, is shown by comparison with the original data (see Figs. 1 and 2).

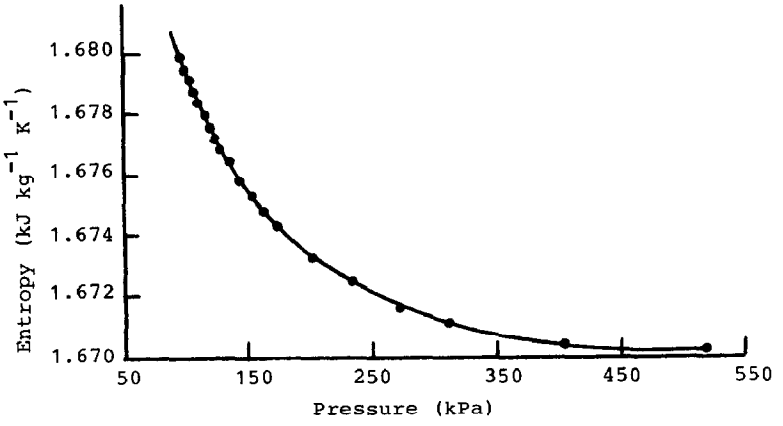

Fig. 1. Curve fitted to vapour entropy data. ($S_v = -1.7 \times 10^{-9}\, P^3 + 9.155 \times 10^{-7}\, P^2 - 2.353 \times 10^{-4}\, P + 1.695$)

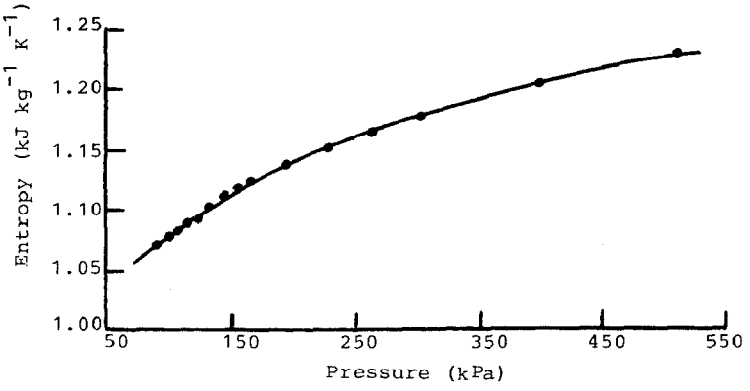

Fig. 2. Curve fitted to liquid entropy data. (S_L = 1.6 × 10^{-9} P^3 − 2.007 × 10^{-7} P^2 + 1.091 × 10^{-4} P + 0.918)

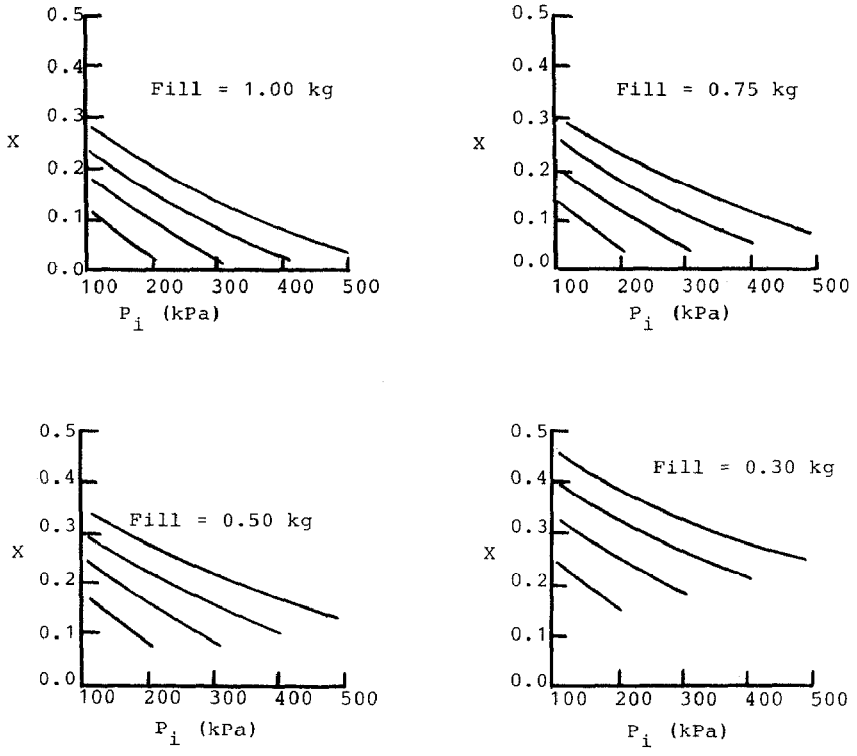

Fig. 3. Theoretical quality curves with varying initial pressure and fill level.

The calculated data for quality is presented in Fig. 3. This figure shows that between 10% and 45% of Freon-11 is vaporised during the expansion. This is supported by the results from the experimental programme described above and by the work of others [1, 3].

However, it is the relationship of these parameters with time, not pressure, which is of most significance. As previously mentioned, there is no simple, theoretical way of converting these pressure dependencies to time dependencies. The experimental work included the production of pressure history data (see Fig. 4) and thus a simple method of relating pressure to time is now available.

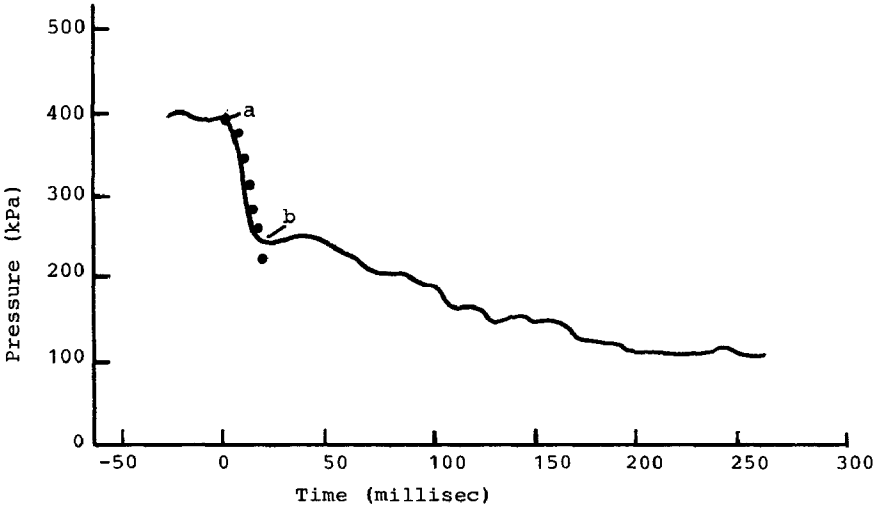

Fig. 4. Experimental pressure history curve. Point (a) corresponds to the beginning of vessel failure, and point (b) to the onset of flash boiling.

A typical pressure history trace is given in Fig. 4 (P = 310.3 kPa, W = 1000 g). The trace can be divided into a number of major sections. Point (a) corresponds to the beginning of vessel failure. This is followed by a rapid fall in pressure, taking 15 to 20 ms. It is suggested that this is due to the exit of vapour from the vessel, and occurs before the flash boiling begins. In several cases there is then a small rise in apparent pressure lasting for a similar time. This pressure is probably due to the impact of liquid on the pressure sensor resulting from the onset of flash boiling. Then, after this "momentum peak" has subsided the pressure falls smoothly to atmospheric, although at a far slower rate than in the initial decay. It is during this period that the two phase release occurs, with the expanding vapour entraining the remaining liquid and carrying it away from the vessel.

It is possible to model the changes, which occur in the pressure history prior to the onset of flash boiling at point (b).

Integrating the continuity equation over the volume V_1 corresponding to the volume occupied by gas in the vessel leads to

$$\frac{d\rho_1}{dt} + \operatorname{div} \rho_1 \vec{U}_1 = 0 \tag{6}$$

$$\frac{\partial}{\partial t}\int_{v_1} \rho_1 \, dV + \int_{v_1} \operatorname{div} \rho_1 \vec{U}_1 dV = 0 \tag{7}$$

By applying Gaussian theory to the second term and assuming that the gas velocity at the vessel wall is zero and that the annular velocity, U, is contant, then

$$\int \operatorname{div} \rho_1 \vec{U}_1 \, dV = \rho_1 U_1 A \tag{8}$$

and

$$\rho_1 = \beta P_1 \tag{9}$$

where $\beta = W_1/RT_1$ = constant.

The pressure of the gas in volume V_1 can be considered constant but will change rapidly on the failure of the vessel, i.e. the change in pressure is considerable while the change in volume is negligible

$$V_1 \frac{dP_1}{dt} = - P_1 U_1 A \tag{10}$$

By taking a hydraulic approximation to the momentum balance, it is possible to introduce a quasi-stationary relationship for the outflow of the jet

$$u_1 = \sqrt{\frac{P_1 - P_A}{\rho_1}} \tag{11}$$

The annular area, A, changes during the process from zero to the area A_e at the time of pressure equalisation. For convenience, this will be described by a power law

$$A = A_e \left(\frac{t}{t_e}\right)^w \tag{12}$$

By substitution of eqns. (11) and (12) into eqn. (10)

$$\frac{\partial p'}{\partial t'} = \sqrt{p'(p' - 1)} \, (t')^w \tag{13}$$

where $p' = \dfrac{P_1}{P_A}$, $t' = \dfrac{t}{t^*}$, and $t^* = \left(\dfrac{\sqrt{\beta}\, V_1}{A_e\, t_e}\right)^{1/(w+1)} t_e$.

Equation (13) describes the rate of the pressure drop. Integration of eqn. (13) with the initial condition of $p' = p'_i$ where

$p'_i = P_i/P_A$ leads to

$$\frac{(t')^{w+1}}{(w+1)} = \ln\left(\frac{2p'_i - 1 + \sqrt{(2p'_i - 1)^2 - 1}}{2p' - 1 + \sqrt{(2p' - 1)^2 - 1}}\right) \tag{15}$$

This equation is only valid for the initial period and cannot be applied for the whole transient process. The value of t^* in eqn. (14) determines the characteristic time of the pressure drop.

Figure 4 also illustrates the correlation between this theoretical approach and the experimental pressure drop for the following conditions:

$V_1 = 0.97 \times 10^{-3}$ m^3, $W_1 = 137.37 \times 10^{-3}$, $T_1 = 300$ K, $t_e = 0.225$ s;

and the assumptions of: $w = 1$, and $A_e = 0.59 \times 10^{-3}$ (corresponding to a final opening of 1.5 mm). Between points (a) and (b) in Fig. 4 good agreement is obtained, however, deviations occur beyond this region as expected.

Theoretical pressure vs. time plots are given in Fig. 5 for different initial pressure values, using $w = 1$.

Figure 6 shows the relationships using different power laws and an initial pressure of 3 bar. If the opening of the vessel is very rapid (if the power exponent w is small) the pressure drops more rapidly.

Previous work on such vessel failures has concentrated solely on the effects outside the vessel. This has not produced results with can be directly compared to this work, where the emphasis is towards a "catastrophic failure" providing a source term for other consequence models.

Work on two-phase releases has largely involved exit from pipes, where most, if not all, of the flash boiling has occurred after the release. In the

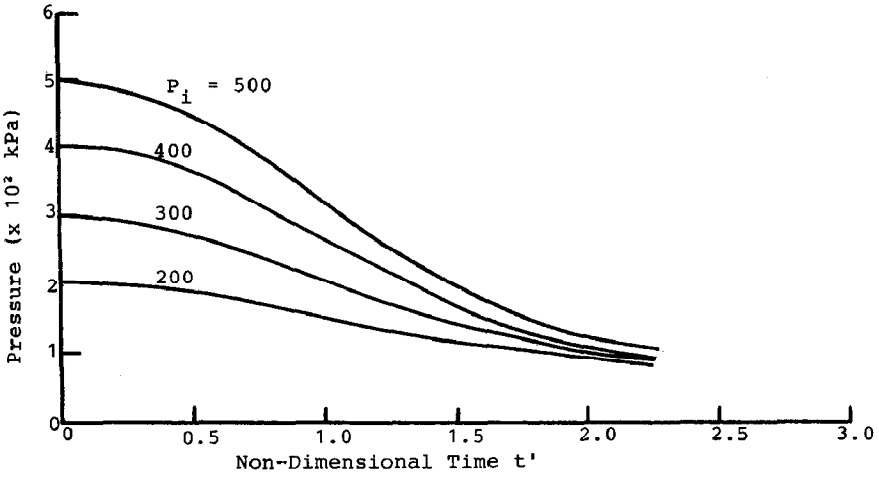

Fig. 5. Theoretical pressure history with varying initial pressure.

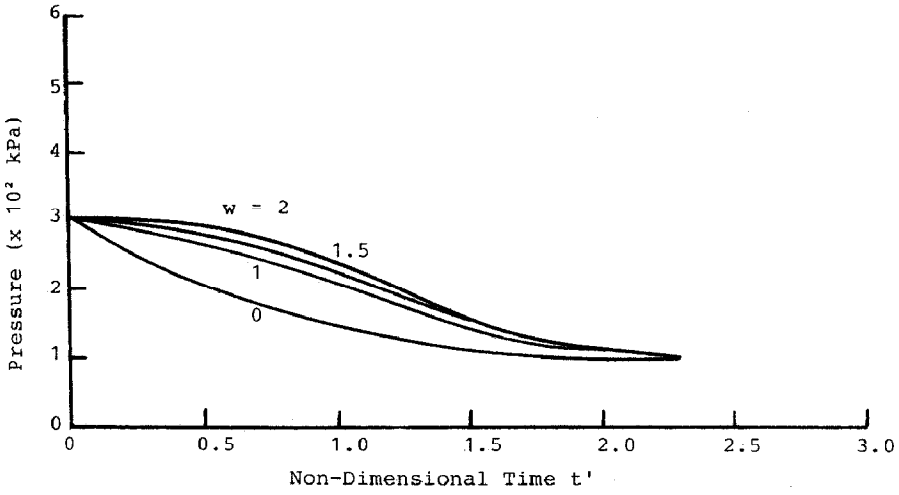

Fig. 6. Theoretical pressure history with varying failure rates.

case of major vessel failure, the flashing will take place inside the vessel, as in the experimental studies described in this paper.

Mathematical model — The latter evolution

A number of different treatments are available for the expansion of the "heavy gas cloud" following the initial stages of the release. The above experimental work is unique in providing the aerosol size characteristics and this allows the use of techniques already developed to deal with particulate clouds.

The model is applicable to particulate cloud motion under gravity in an unconfined medium, i.e. the atmosphere. It is based on dynamic, two-dimensional equations for unconfined multi-phase mechanics.

The final stage of cloud evolution is assumed to start when the particles have reached their maximum height. At this point they can be described as a cloud of stationary, mono-sized, spherical particles suspended above the ground. The particles then start to move downwards under gravity, giving rise to gas movement. It is necessary to follow the movement of the particles and gas until all the particles have reached the surface.

The main assumption of multi-phase mechanics is that the diameter of the particles and the mean distance between the particles are much smaller than the distance over which there is a significant change in the macroscopic parameters [11]. The system under investigation can be considered as two intermixed interacting media, the gas and the particles. The diameter of the particles is much larger than the molecular/kinetic scales.

In the following treatment, Brownian motion, evaporation and break-

up of the particles are neglected, although it is recognised that these may be of considerable importance, particularly evaporation.

A cloud with small particulate volume fraction ($\alpha_2 \ll \alpha_1$) will be considered. The ratio of the actual gas and particle density is assumed small

$$\frac{\rho_1}{\rho_2} \ll 1$$

Based on initial cloud radius, r, non-dimensional variables can be defined:

velocity = $\sqrt{gr}$

time = $\sqrt{r/g}$

Two dimensional motion of the mixture can be described by

$$\frac{d_j \rho_j}{dt} = -\rho_1 \operatorname{div} \vec{U}_1 \tag{16}$$

as $\rho_1 \propto P$ in the isothermal case

$$\rho_1 \frac{d_1 U_1}{dt} = -\frac{1}{\gamma M^2} \operatorname{grad} P + \vec{P_g} + \frac{1}{\mathrm{Re}} (\Delta \vec{U} + {}^1/_3 \operatorname{grad} \operatorname{div} \vec{U}_1) - \vec{f} \tag{17}$$

note

$$\vec{g} = \{0, -g\}$$

$$\frac{d_2 \rho_2}{dt} = -\rho_2 \operatorname{div} \vec{U}_2$$

$$\rho_2 \frac{d_2 \vec{U}_2}{dt} = \rho_2 \vec{g} + \vec{f} \tag{18}$$

note that $\rho_j = \rho_{ji}\, \alpha_j$

$$\frac{d_j}{dt} = \frac{\rho}{\rho t} + (\vec{U}_j\, \vec{U}) - \text{substantial derivatives}$$

The dynamic viscosity, η, is assumed constant. The evolution of the cloud can be considered to be an isothermal process, since the heating of the system due to the viscous energy dissipation is small and both gas and air temperatures can be considered to be held at the initial temperature, T_i.

Both planar (see Ref. [12]) and axi-symmetrical cases can be considered. For the planar case, it is assumed that the cloud size is greater in one horizontal direction than the other. The force for interaction at the interface is defined by

$$\vec{f} = \frac{3}{4} \frac{\epsilon}{\delta} C_d \, \mathrm{Re}_p \frac{\rho_1 \rho_2}{1 - \alpha_{2i}} | \vec{U}_1 - \vec{U}_2 | (\vec{U}_1 - \vec{U}_2) \tag{19}$$

where

$$C_d = \frac{24}{Re_p}(1 + 0.158\ Re_p^{0.5})$$

$$Re_p = Re_{pi}\,|\,\vec{U}_1 - \vec{U}_2\,|\,\frac{\rho_1}{\alpha_1}$$

The origin for the coordinates in situated under the cloud mass centre, the x-coordinate being along the ground and the y-coordinate along the plane of symmetry for the planar case and along the axis of symmetry for the axi-symmetrical case.

Initially, the stationary gas is in a static equilibrium with a cloud of stationary particles and a Gaussian distribution of particle concentration is applicable

$$N_i = \exp\,[-(x^2 + (y - H)^2)]$$

and

$$\rho_2 = \frac{\alpha_{2\,i} N}{\epsilon}$$

$$\text{i.e., } x = 0,\ U_i = 0,\ \frac{\partial U_1}{\partial x} = 0,\ \frac{\partial P_i}{\partial x} = 0$$

$$x^2 + y^2 \to \infty,\ U_1 = 0,\ \frac{\partial P}{\partial y} = -\gamma M^2 \rho,\ y = 0,\ \vec{U} = 0$$

The boundary conditions take into account the symmetry about the plane $x = 0$; and the equilibrium state at infinity. Particles which reach the ground play no further part in the process.

Taking values for the parameters based on data from the initial expansion stage:

$n_i = 10^3\ \text{cm}^{-3}$, $\alpha_{2i} = 10^{-3}$, $M^2 = 0.72 \times 10^{-3}$, $\gamma = 1.4$, $\epsilon = 10^{-3}$;

for the particles:
total mass of particles = 1000 g, density $\rho_2 = 1000\ \text{kg m}^{-3}$; and for air: density $\rho_1 = 1.3\ \text{kg m}^{-3}$, $\eta/\rho_1 = 1.4 \times 10^{-5}\ \text{m}^2\ \text{s}^{-1}$, $T_i = 300$ K, and $r = 1$ m. The terms which depend on particle size have the following ranges:

$\delta = 3.3 \times 10^{-6} \to 2 \times 10^{-4}$ $\qquad$ $H = 1.5 \to 14$

$Re = 7 \to 60\alpha_{2i}\ 10^{-3} \to 10^{-2}$ $\qquad$ $Re_{pi} = 6.5 \times 10^6\ \delta = 21.4 \to 1300$

The external Reynolds' numbers are large, indicating turbulent motion, and are estimated using an effective viscosity. The particles are very small in comparison with the scale of turbulence and the Reynolds' number for the particles uses a molecular viscosity, i.e. the Reynolds' numbers for gas and particle are independent. Numerical methods for the solution of

this problem have been developed [13] and two regimes of cloud evolution can be considered.

The interaction with the ground begins when the height of the cloud centre is equal to or approaching twice the radius of the cloud. The movement of the cloud can be considered to be unconfined between the initial release and reaching the surface.

The stationary particles start to move downwards under gravity. The entrainment of the surrounding gas due to friction is described by an emperical law (eqn. (19)). The effect of entrainment increases with decreasing distance between the particles (i.e. increasing particle concentration). In this case hydrodynamic interaction occurs between the particles throughout the cloud as a result of large scale motion of the air. The velocity of the cloud increases continuously and exceeds that of a single particle. This is called the "entrainment" regime.

If the distance between the particles is sufficient, each particle behaves as a single free-falling sphere because it is unaffected by any gas motion caused by the other particles. This is called the "filtration" regime because the gas filters through the particles.

The different regimes of cloud motion are presented in Fig. 7, in which the vertical movement of the cloud centre with time is shown for various values of α_{2i} and constant values of $\delta = 6.67 \times 10^{-5}$ and Re = 29.05. It should be noted that this value for the external Reynolds' number is used in all calculations below. Where interaction with the surface occurs, this is indicated by dotted lines. All the curves lie between curve A which corresponds to frictionless motion and a free-fall law ($y = H - t^2/2$), and the curve which corresponds to the fall of a single particle in the air.

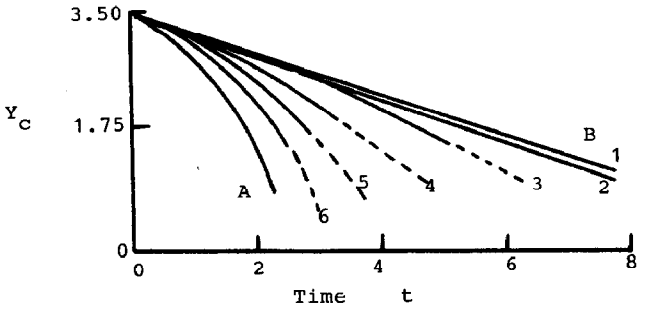

Fig. 7. Time dependence of cloud centre with varying particle concentrations.

Curve B can be produced by integrating the equation of motion, which can be expressed in a non-dimensional form as

$$\frac{dC}{dt} = -1 + \frac{3}{4}\frac{6}{8} \exp(-\gamma M^2 y)\, C_d\, Re_p\, C^2$$

where $C = dy/dt$ with the initial conditions $y_i = H$, $C_i = 0$.

In the planar case, for low particle concentrations (giving the "filtration" regime) the motion of the cloud coincides with that of a single particle (curves 1 and 2). An increase in particle concentration (α_{2i}) leads to stronger interaction and the cloud velocity rises. The motion tends to that of frictionless free-fall, curve A. Curves 3 to 6 correspond to the "entrainment" regime.

A change of regime occurs when the ratio of particle diameter to cloud radius is varied. The boundary between the two regimes in the planar case is decribed by

$$\ln \alpha_{2i} = (0.825 \times 10^4)\,\delta - 4.56 \qquad (20)$$

to within 7% accuracy for the ranges $3.3 \times 10^{-5} \leqslant \delta \leqslant 2 \times 10^{-4}$ and $10^{-5} \leqslant \alpha_{2i} \leqslant 10^{-2}$.

It is assumed that the filtration regime occurs when $C/(\mathrm{d}y/\mathrm{d}t) \leqslant 1.2$. At a fixed value of δ, the "filtration" regime occurs if the parameter α_{2i} is small.

In the "filtration" regime, as every particle moves individually, the initial cloud shape does not change. In the "entrainment" regime the cloud shape changes continuously.

At first, the lines of equal particle concentration form concentric circles. The cloud is similar to a drop moving through a liquid, i.e. the particles move downwards in the centre of the cloud and move upwards near the edge. With time and an increasing cloud velocity, the "drop" is deformed. A "dimple" forms in the bottom of the "drop". Gradually the drop transforms into the "cap" previously described by other workers [14, 15, 16].

The gas zone is increasing continuously. Large scale vortex motion is formed, causing lateral displacement of the particles. The zones with greatest particle concentration are moved from the cloud centre (plane $x = 0$, in the axi-symmetrical case). As a result, the lines of equal concentration break-off at a definite time.

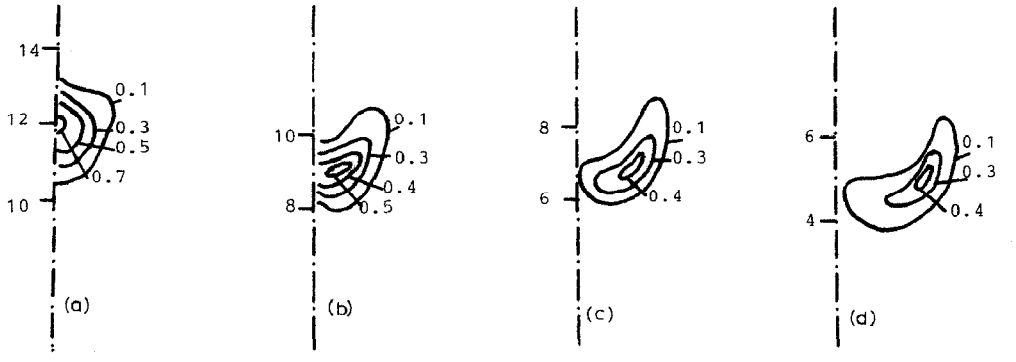

Fig. 8. Cloud evolution in the "entrainment regime". The flow field and lines of equal concentration are presented at various times: (a) 4.16, (b) 6.94, (c) 9.71 and (d) 12.5.

Two symmetrical cylindrical vortices with the particles in their core are formed in the planar case (or a toroidal vortex in the axi-symmetrical case). The evolution of the cloud is shown in Fig. 8. The flow field and lines of equal concentration are presented for $\alpha_{2i} = 10^{-3}$ and $\delta = 6.67 \times 10^{-5}$ at various times, i.e. (a) 4.16, (b) 6.94, (c) 9.71, (d) 12.5.

The process of evolution of the cloud can be followed experimentally by noting the changes in shape.

Characteristics of sedimentation

In the filtration regime all the particles are descending vertically on direct line trajectories. The interaction obviously does not depend on the initial cloud height.

The distribution of the particles falling on the surface can be determined analytically by means of integration of the initial particle distribution over coordinate y

$$n_s(x) = \int_0^\infty n\,(x, y, \mathrm{i})\,dy$$

$$= \sqrt{\pi}/2\,[1 + \mathrm{erf}\,(H)]\,\exp\,(-x^2)$$

where n_s = dimensionless concentration of particles on the surface. For $H \gg 1$, $n_s = \sqrt{\pi}\exp(-x^2)$.

In the "entrainment" regime the large scale vortex motion leads to lateral displacement of the particles above the surface. Therefore, the particles are scattered across the surface. The scattering increases with increasing initial cloud height. The cloud profile at various times during sedimentation is shown in Fig. 9. These profiles are based on the conditions: $\alpha_{2i} = 10^{-3}$, $H = 4.8$, and $\delta = 6.67 \times 10^{-5}$.

It is possible to identify the formation of: (a) the vortex flow structure, (b) the "cap", (c) the deformation of cloud shape during sedimentation, and (d) gas propagation across the surface and the scattering of particles.

The vortex motion across the surface leads to characteristic distribution curves. Initially, the particles land near the line of symmetry. Then the fall-out takes place at a certain distance. The final distribution gives a maximum located some distance from the central line and a considerable number of particles can fall on the surface outside the initial projection of the cloud.

This effect can be estimated quantitatively by introducing a coefficient for scattering on the surface. This coefficient is equal to that fraction of the particles which lands outside the initial geometrical "shadow" of the cloud on the ground.

$$e = 1 - N_s/N \tag{22}$$

where N = total number of particles, N_s = number of particles landing outside the initial cloud projection.

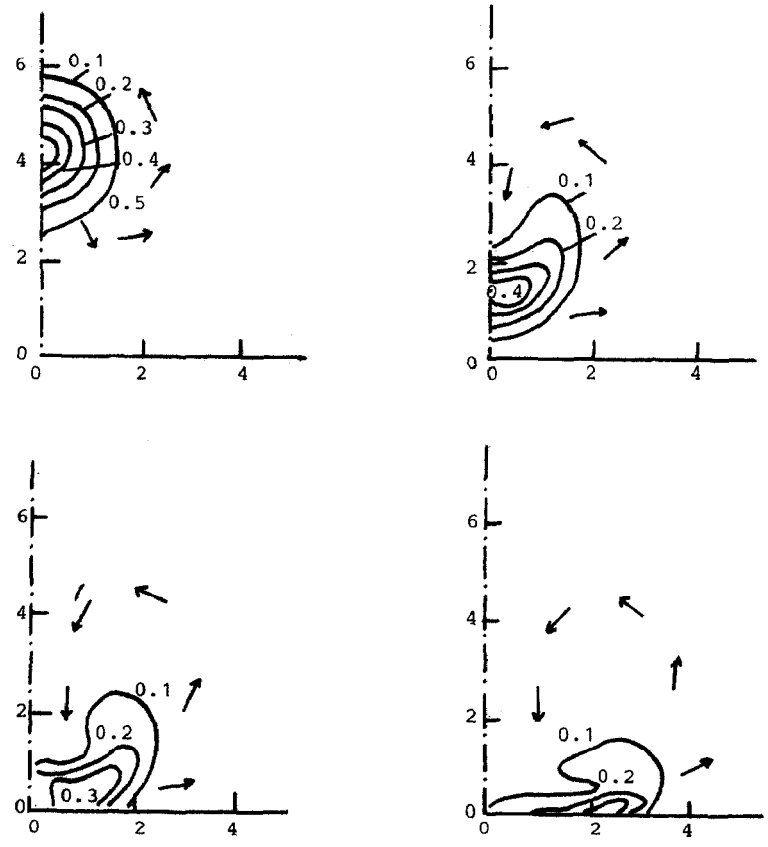

Fig. 9. Cloud sedimentation on the surface at various times.

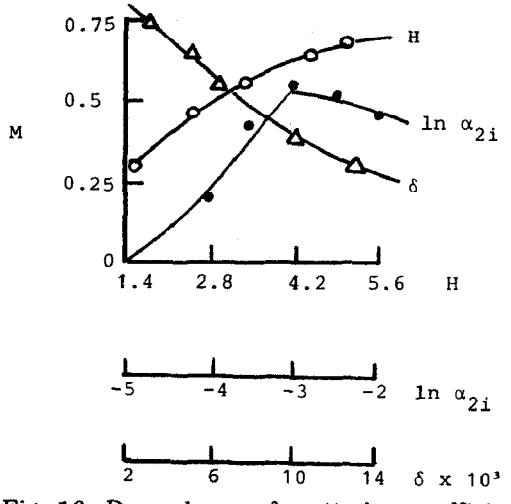

Fig. 10. Dependence of scattering coefficient on particles size (δ), concentration (α_{2i}) and initial level (H).

In the "filtration" regime, the coefficient is near to zero. In the "entrainment" regime, the scattering depends on several parameters (e.g. H, δ and α_{2i}). The effect of each of these is shown in Fig. 10.

With increasing initial height, H, the scattering increases, as the vortex motion takes place in a larger volume and the particles move a considerable distance from the centre-line, $x = 0$ (in Fig. 10, $\alpha_{2i} = 10^{-3}$ and $\delta = 6.67 \times 10^{-5}$).

With increasing particle size, δ, the scattering diminishes, as the smaller particles are more easily entrained into the vortex motion (in Fig. 10, $\alpha_{2i} = 10^{-3}$ and $H = 3.373$).

If α_{2i} is increased, then the scattering initially increases, marking the transition from "filtration" to "entrainment" regimes. However, scattering then decreases, as the increase in vertical velocity means that the particles fall too rapidly to move far from their initial positions relative to the cloud centre. (In Fig. 10, $H = 3.373$ and $\delta = 6.67 \times 10^{-5}$.)

Throughout this work an isothermal mixture has been assumed. This is a reasonable approximation since the boiling point of Freon-11 at normal pressure is not significantly different to ambient temperature. However, for other hydrocarbons the temperature difference in liquid and gaseous phases may be significant.

Conclusions

Physical and mathematical modelling has been used to investigate the separate stages of the release of a two-phase mixture from a pressurised vessel. This has provided a methodical basis for the further study of the individual stages and of the process as a whole.

In order to study the first stage of such processes, experiments have been conducted on the "failure" of a vessel filled with liquid Freon-11. Data was obtained for the size and velocity of particles, pressure equalisation time and the time dependence of the pressure in the vessel. An analysis of the experimental data combined with thermodynamic data has allowed a definition of the time dependence of the process.

The assumption that the process is isentropic, despite only approximating to the actual nature of the process, provides satisfactory and reasonable results. The results obtained can be used to estimate the parameters of the cloud formed during the failure of a pressurised vessel.

Continued study of the first stage is of interest, as many questions have not yet been investigated. Among these questions are:

1. Concentration profiles within the vapour as air entrainment takes place requires investigation.
2. The study and comparison of the release characteristics of different materials, including the release of solid particles and also mixtures of solids and liquids.
3. The development of a theory for the expansion of the release which

can describe the process as a whole, without the need for relationships based purely on experiment.

4. The investigation of flow patterns and temperature distributions set up during the release, for both the particles and the vapour, thus giving an insight into these irreversible processes which occur during the release. This will allow theories developed in the future to be based on the most realistic assumptions.
5. The investigation of the cloud formation with simultaneous combustion inside the vessel.

The later stage of cloud evolution has been studied by using mathematical modelling. The mathematical formulation of the cloud evolution has been based on the two phases having separate velocities.

The character of the cloud motion has been shown to depend upon the extent of the hydrodynamic interaction which occurs between the particles via the gaseous phase.

For a small volume fraction of particles this interaction is not so large, and each particle behaves as a single particle (the "filtration" regime). If the concentration of the particles is high enough the air between the particles is entrained by the particle motion; as a result the cloud velocity exceeds that of a single particle. In the "entrainment" regime large scale vortex motion arises; the cloud is transformed into two cylindrical vortices in the case of planar symmetry. The regime of cloud motion defines the features of the sedimentation of the particles on the horizontal surface. In the "entrainment" regime, the particles entrained into the vortex motion move laterally, therefore they sediment over some distance.

For the future development of this theory, it would be of interest to consider the following questions:

1. The evaporation of the particles, and taking into account the temperature difference between the gas and the particles. This is especially important for the study of LPG-releases.
2. The combustion of the cloud above the vessel.

It can be noted that a methodical basis for considering non-isothermal cases already exists [17, 18].

As for the intermediate stages of the considered processes, it will be useful to develop the mathematical modelling of these stages and to apply the self-similar solutions for the jet-like flows.

Acknowledgements

The authors would like to express their gratitude to N. Kidin for his help in the formulation of the pressure—time relationship (eqns. (10) and (11)). They also wish to thank the Health and Safety Executive for their financial support and helpful advice with regard to the experimental work.

List of symbols

Main symbols

A exit area
C cloud acceleration
d particle diameter
e coefficient of scattering
g gravitational acceleration
H height above surface
m molecular weight
N number of particles
n particle concentration
P pressure
R gas constant
r cloud radius
S entropy
T temperature
t time
U,u velocity
V volume
W total mass of release
X quality (vapour mass fraction)
x,y geometrical coordinates
α volume fraction of particles
γ specific heat ratio
δ relative diameter of particles = d/r_i
ϵ density ratio = ρ_1/ρ_2
η dynamic viscosity
ρ density
w power term for vessel failure

Groups

C_d drag coefficient
f drag force
M Mach number
p' non-dimensional pressure
Re Reynolds number
t' non-dimensional time
t^* characteristic equalisation time
β release characteristic = W/RT

Subscripts

A of the atmosphere
e at pressure equalisation
i at the initial state

p of particles
s on the surface
t at a moment in time
1 vapour phase
2 liquid/solid phase
j of one component

Note: A vector quantity is indicated with the symbol → above it, e.g. $\vec{U}$. The vector operations are indicated as Δ, grad and div

References

1 H.C. Hardee and D.O. Lee, Expansion of clouds from pressurised liquids, Accid. Anal. Prev., 7 (1975) 91—102.
2 P.F. Nolan and J.A. Barton, Runaway reactions in batch reactors, IChemE., Symp. Ser. 85, Chester, 1984.
3 H. Giesbrecht, K. Hess, B. Maurer and W. Leukel, Explosion hazard analysis of inflammable gas released spontaneously into the atmosphere, Chem. Ing. Techn., 52(2) (1980) 114—122.
4 K. Sato and K. Hasegawa, Study on the fireball following steam explosion of n-pentane, Second International Symposium on Loss Prevention and Safety Promotion in the Process Industries, European Federation of Chemical Engineers (E.F.C.E.), 1977.
5 R.E. Britter and R.F. Griffiths, The role of dense gases in the assessment of industrial hazards, J. Hazardous Materials, 6 (1982) 3—12.
6 P. Field, Dust explosion protection, J. Hazardous Materials, 8 (1984) 223—238.
7 F.P. Lees, Loss Prevention in the Process Industries, Butterworths, 1980.
8 D.R. Blackmore, M.N. Herman and J.L. Woodward, Heavy gas dispersion models, J. Hazardous Materials, 6 (1982) 107—128.
9 J.L. Woodward, J.A. Heavens, W.C. McBridge and J.R. Taft, A comparison with experimental data of several models for dispersion of heavy vapour clouds, J. Hazardous Materials, 6 (1982) 161—180.
10 Kuzman Raznjevic, A Handbook of Thermodynamic Tables and Charts, McGraw-Hill Book Co., New York, 1976.
11 R.I. Nigmatulin, Osnowy Mechaviki Getterogennych Sred, M. Nauka, 1978, 336 pp.
12 G.M. Makhviladze and O.I. Melichov, On the cloud motion and sedimentation under gravity above a flat horizontal surface, Izvestia USSR Academy of Sciences, Liquid and Gas Mechanics, 6 (1982) 64—73.
13 G.M. Makhviladze and S.B. Tscherbak, Numerical methods for the investigation of non-stationary spatial motions of pressurised gas, J. Eng. Phys., 38(3) (1980) 317—323.
14 G.W. Slack, Sedimentation of compact clusters of Uniform Spheres, Nature, 200 (1963) 466—467.
15 G.W. Slack, Sedimentation of a large number of particles as a cluster in air, Nature, 200 (1963) 1306.
16 K. Adachi, S. Kiriyama and N. Yoshioka, The behaviour of a swarm of particles moving in a viscous fluid, Chem. Eng. Sci. 33 (1978) 115—121.
17 G.M. Makhviladze and O.I. Melichov, On the motion and evolution of cloud with initially hot particles, Doklady USSR Academy of Sciences, 267(4) (1982) 844—847.
18 G.M. Makhviladze and O.I. Melichov, Combustion of an aerosol cloud above a flat horizontal surface, Chem. Phys., 7 (1983) 991—998.